Molecular motion in solid H_2 at high pressures

Sam-Hyeon Lee, Mark S. Conradi, and R. E. Norberg
Department of Physics, Washington University, St. Louis, Missouri 63130
(Received 10 August 1989)

Solid molecular hydrogen has been studied with proton nuclear magnetic resonance in a diamond anvil cell. Pressures from 18 to 68 kbar were used, resulting in melting temperatures from 160 to 350 K and relative densities ρ/ρ_0 as high as 3. At temperatures above $0.7T_{melt}$, translational self-diffusion narrows the resonance line. The pressure variation of the activation enthalpy ΔH yields an activation volume of 5.7 ± 0.6 cm^3/mol or 63% of the molar volume, a reasonable value for a vacancy diffusion mechanism. The smooth variation of $\Delta H/kT_{melt}$ with density also suggests that the diffusion mechanism remains the same for ρ/ρ_0 between 1 and 3. The spin-lattice relaxation is controlled primarily by molecular reorientation. The observed density dependence $T_1 \propto \rho^{5/3}$ indicates that molecular electric quadrupole-quadrupole interactions cause reorientation, even at the high temperatures and densities of this work.

I. INTRODUCTION

In recent years there has been substantial interest in the behavior of molecular solids at high pressures and densities. Much work on structural phase transitions using x-ray diffraction[1–3] and Raman spectroscopy[4–7] has been reported. Optical techniques[8,9] and dc resistance measurements[9] have been used to study insulator-metal transitions. Recently, we reported the feasibility of nuclear magnetic resonance (NMR) experiments in a diamond anvil cell (DAC).[10] Using the sensitivity of NMR to molecular motions, we have studied and report here the effects of high pressure on self-diffusion and molecular reorientation in solid H_2.

The effects of pressures up to 68 kbar upon solid H_2 are profound. The melting temperature (see Fig. 1) varies from 14 K at essentially zero pressure (the lowest triple temperature of any substance) to 350 K at 68 kbar,[11] a factor of 25 increase. Over this pressure range the density[12,13] increases by a factor of 3. The large compressibility of solid H_2 arises in part from the small number of electrons and the correspondingly small repulsion term. Also, at low pressures the volume of condensed H_2 is expanded by zero-point motion, which is large because of the small mass. The large changes in T_{melt} and density in H_2 may be contrasted with the smaller effects of 70 kbar upon solid N_2: a factor of 8 increase in T_{melt} and 1.7 increase in density.[3]

Self-diffusion in most solids at normal densities occurs through the monovacancy mechanism.[14] This mechanism naturally has a large activation volume ΔV, which increases the activation enthalpy $\Delta H = \Delta E + P\Delta V$ at high pressures. One may expect at sufficiently high pressures that some other mechanism with a smaller ΔV will become the dominant diffusion mechanism. For example, ring exchange (interchange) occurs via quantum tunneling[15] in solid He^3. Ring exchange has also been discussed as a possible classical diffusion mechanism of silicon[16–18] and graphite.[17] We have examined our H_2 diffusion data for a change in mechanism; we find no such evidence.

In molecular solids, it has been observed that the diffusion rate in the solid at the melting point is a constant, independent of pressure.[19] Because only small changes in the diffusion prefactor occur, this implies that the ratio of the activation enthalpy to the melting temperature stays constant. This has been studied previously

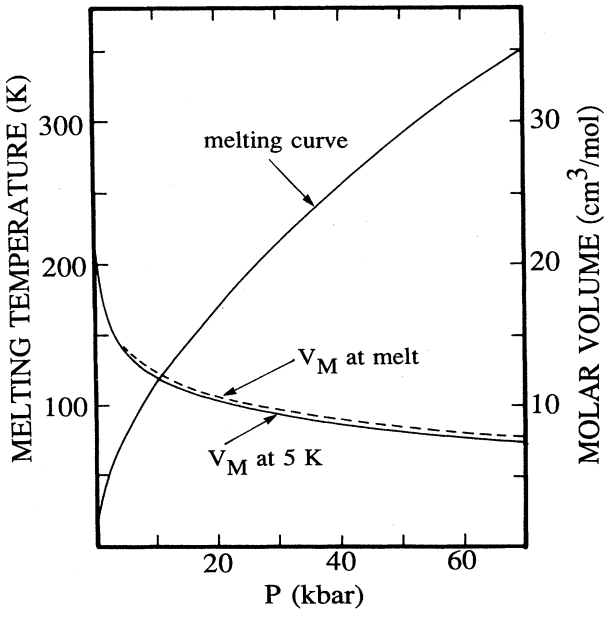

FIG. 1. The pressure variation of the melting temperature and the molar volume of H_2. The solid curve is for 5-K molar volume and the dashed curve refers to the solid at the melting point. The values are taken from Refs. 11–13 with some small extrapolations for melting point volumes and the melting temperatures.

with modest pressures producing only 30% changes in T_{melt}. The H_2 data reported here test this empirical relation over a much wider range of conditions.

At low temperatures and pressures, ortho-H_2 molecules are in the $J=1$ state and are the only specie with nonzero nuclear spin.[20] The ortho-H_2 may be regarded as a system of molecular spins-one coupled by their electrical quadrupole-quadrupole (EQQ) interactions. This model is very successful in explaining molecular reorientation and the resulting nuclear spin relaxation[21] in solid H_2. By contrast, our study involves temperatures as high as 330 K, so higher J states will be present. Further, coupling between phonons and molecular orientations may be important at the high temperatures. Finally, at high density one expects that shorter-range anisotropic molecular repulsion and attraction terms may couple the molecular orientations, in addition to the EQQ coupling. These effects are examined in the nuclear spin relaxation data of H_2 at high pressures, as reported here.

II. EXPERIMENTAL METHODS

Some techniques for NMR in a diamond anvil cell have been described previously.[10] The essential feature is to apply a rf field H_1 parallel to the metallic gasket so that H_1 penetrates into the gasket hole. Here we use a copper ribbon resonator, a one-turn coil resonating with a small chip capacitor. The current path is physically small to improve the filling factor, which nevertheless is only about 10^{-2}. Adjustable tuning and coupling capacitors are located nearby and transform the impedance to 50 Ω. The capacitors are adjusted from the room via long extension shafts. For high sensitivity the experiments are performed at 340 MHz in an 8-T superconducting solenoid. An important feature of the ribbon resonator is that it can be cleaned in acetone with ultrasound to remove finger grease, etc. (the H_2 samples are ~ 4 μg and stray proton signals must be avoided).

The NMR spectrometer is of conventional design. The ~25-W output power results in a $\pi/2$ pulse length of 7 μs. The signal-to-noise ratio of single transients is ~2, depending on bandwidth, and is adequate for tuneup. Signal averaging of ~200 transients is generally used for quantitative data.

The DAC (Refs. 22 and 23) is constructed of titanium alloy (6% Al, 4% V) (Ref. 24) and uses a piston and cylinder as a guide for stable alignment. The force required to clamp the gasket and trap a H_2 sample is generated by a single 8-32 screw. For pressures above 30 kbar a lever system is used that fits into the narrow 54-mm magnet bore. The diamonds are $\frac{1}{4}$ carat each, with 1-mm culets. The 0.25-mm-thick gasket is used without preindentation; the gasket hole is 0.5 mm diameter. Hardened Be-Cu is used below 35 kbar and rhenium is used for higher pressures.[25,26] Temperatures are controlled by thermostatted, flowing N_2 gas. The temperature is measured with a thermocouple. We intend to publish more details of the NMR DAC separately.

The fluorescence of a ruby chip is used to measure the presure.[27] An argon ion laser and monochromator are coupled to the DAC by a single 0.1-mm-diam graded index optical fiber with coupling lenses. Our intention was to measure the pressure *in situ,* but the 8-T field broadens the ruby spectrum. We resorted to measuring the pressure outside the magnet in a separate temperature controlling apparatus. Correction for the temperature shift of the ruby spectrum is performed.[28] A typical variation of pressure with temperature appears in Fig. 2. The pressure is nearly constant in the solid, but increases upon melting. This pressure rise is due to the approximately constant volume conditions. The observation of sharp ruby fluorescence lines implies that the pressure is nearly hydrostatic.

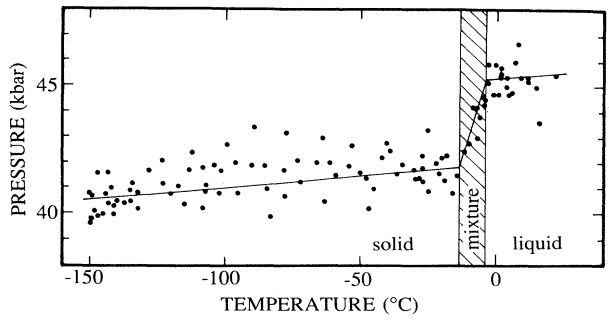

FIG. 2. Typical variation of pressure with temperature, as determined from ruby fluorescence. The temperature interval of H_2 melting is indicated.

Hydrogen is loaded by placing the DAC without its lever system into a conventional pressure vessel.[29] H_2 gas at 400 bars directly from a commercially available cylinder is introduced into the pressure vessel at 77 K. The density of H_2 under these conditions is approximately equal to that of normal liquid H_2. The DAC is closed using an O-ring sealed screwdriver.

III. RESULTS AND DISCUSSION

The spin-spin relaxation time T_2 was determined from free induction decays (FID's) for $T_2 \lesssim 75$ μs. The pulse sequence of Carr, Purcell, Meiboon, and Gill (CPMG) was used for longer T_2.[30] The presence of liquid H_2 was indicated by a substantial increase in T_2. Also, in the liquid phase only, the apparent T_2 from the CPMG experiment increased as the pulse separation was decreased. This behavior indicates rapid diffusion through the magnetic field gradient.[30] For liquid H_2, the FID had a decay time T_2^* of ~900 μs with Be-Cu gasket, presumably arising from the magnetic susceptibilities of the gasket, diamonds, and ruby chip. Rhenium gaskets gave a considerably shorter value, $T_2^* \simeq 100$ μs.

The T_2 measurements for solid H_2 at several pressures are plotted in Fig. 3 as a function of reciprocal temperature. As temperature increases, the line is narrowed and T_2 is increased by motional narrowing from self-diffusion. For some samples the rigid lattice limit was studied. Other samples suffered from proton-bearing contamination (e.g., finger grease); for these samples the H_2 signal could be distinguished only when the H_2 was motionally narrowed. During the course of the research,

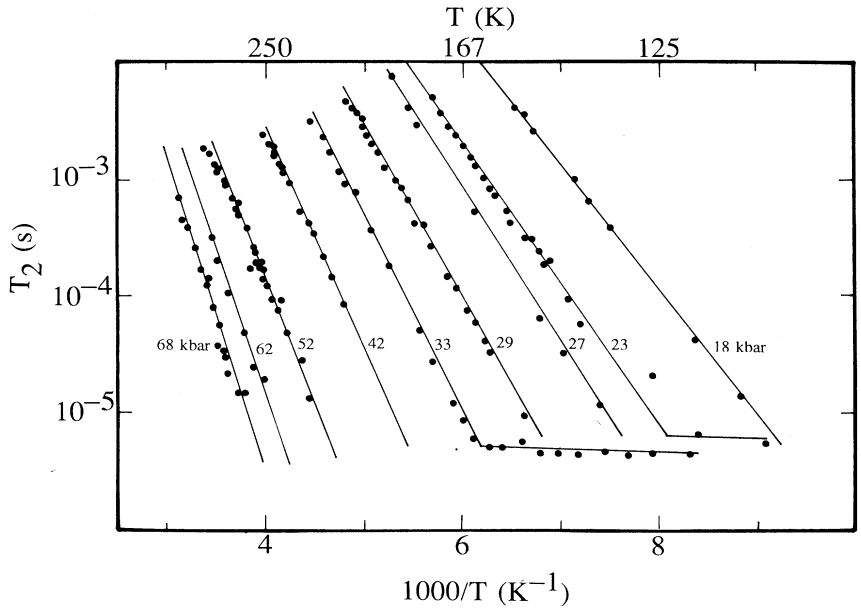

FIG. 3. Transverse relaxation time T_2 of solid H_2 as a function of reciprocal temperature. The numbers on each line label the pressure in kilobars. Self-diffusion motionally narrows the line and increases T_2 as temperature increases. The activation enthalpy derived from the slope increases with pressure (see Figs. 4 and 5 and Table I).

we became more successful in cleaning away contaminants.

The slopes of the lines fit to the motionally narrowed data in Fig. 3 directly yield the activation enthalpies ΔH in Table I. That is, we can write

$$T_2 = T_2^{\infty} \exp(-\Delta H/kT) , \quad (1)$$

because the observed T_2 is proportional to the rate ω_j of molecular diffusion jumps.[19,30] The values of T_2 extrapolated to infinite temperature are T_2^{∞} and depend only weakly upon pressure (Table I).

In the theory of thermally activated processes,[14] the activation enthalpy ΔH is expressed as $\Delta H = \Delta E + P\Delta V$, with ΔE and ΔV constant over a range of temperature and pressure. The pressure variation of ΔH is presented in Fig. 4. The dashed curve schematically connects the high-pressure data of this work to the low-pressure results of Ref. 31. The slope of the straight line fit to the high-pressure data yields $\Delta V = 5.7 \pm 0.6$ cm^3/mol. This ΔV is about 63%±7 of the molar volume V_M of the 40-kbar solid at the melt,[12,13] chosen as the middle of the pressure range studied. We note that the molar volume changes by ~30% from 20 to 70 kbar, so only a slight curvature is expected in Fig. 4, assuming ΔV to be a fixed fraction of V_M.

In pure metals, the diffusion mechanism is certainly monovacancy.[14] Activation volumes, expressed as a fraction of the molar volume, range from 0.33 for tin[32] to 1.35 for aluminum.[14] The alkali metals have values near 0.5 and gold, silver, and lead have values near 0.8.[14] In the case of gold, the activation volume for vacancy migration was found to be much smaller than the diffusion activation volume. Thus most of the diffusion activation volume is associated with vacancy formation. In most molecular (organic) solids, diffusion is also believed to be a monovacancy process.[33] The ratio of diffusion activation volume to molar volume ranges from 0.57 to

TABLE I. Measured and derived parameters of H_2 self-diffusion.

Pressure (kbar)	0	18	23	27	29	33	42	52	62	68
Density, ρ/ρ_0	1	2.15	2.23	2.40	2.45	2.55	2.73	2.86	2.93	2.95
T_{melt} (K)	14	159	183	202	210	227	261	296	328	350
ΔH (K)	190[a]	2480	2770	3040	3400	3790	4320	5030	5650	6140
$\Delta H/T_{melt}$	13.6	15.6	15.1	15.0	16.2	16.7	16.6	17.0	17.2	17.5
Theoretical M_2 (10^{10} s^{-2})	0.24	1.11	1.19	1.38	1.44	1.56	1.79	1.96	2.06	2.09
T_2^{∞} (10^4 s)	0.31[a]	4.7	3.3	7.1	6.9	8.5	8.7	6.8	9.8	15.0
ω_j^{∞} (10^{14} s^{-1})	0.07	4.8	3.6	9.0	9.2	12.2	14.4	12.3	18.6	28.9
T_2^{melt} (ms)	4.0[a]	7.9	8.8	20.7	6.4	4.8	5.6	2.8	3.2	3.6
ω_j^{melt} (10^7 s^{-1})	0.89	8.1	9.7	26.3	8.5	6.9	9.2	5.1	6.1	6.9

[a]Reference 51.

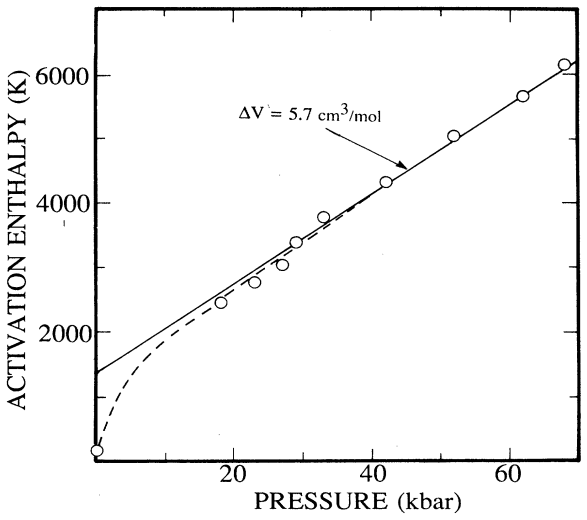

FIG. 4. Activation enthalpy of self-diffusion ΔH in solid H_2 as a function of pressure. The slope of the line through the data yields an activation volume ΔV of 5.7±0.6 cm^3/mol. The dashed curve schematically connects the high-pressure data of this work with a low-pressure datum from Ref. 31.

1.2.[19,34–37] The value reported here for H_2 at high pressures, 0.63±0.07, is at the low end of the range of previous values. A much smaller value would be expected for interstitial mechanisms[32] or the direct exchange mechanism. The measured value indicates that diffusion in high-pressure H_2 occurs through vacancies.

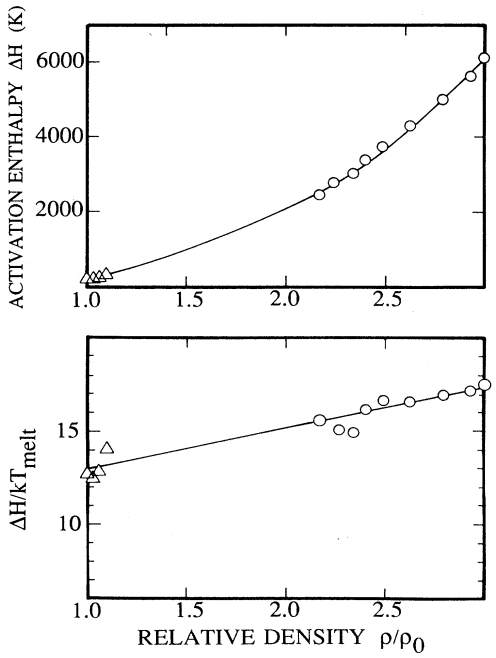

FIG. 5. Activation enthalpy of self-diffusion ΔH as a function of relative density. The density ρ_0 refers to H_2 at 4.2 K and 1 bar. The high-density data (circles) are from this work and the low-density data (triangles) are from Ref. 31. The ratio $\Delta H/kT_{melt}$ also is displayed.

The density dependence of the activation enthalpy ΔH appears in Fig. 5. The high-density data of this work and previous low-density data[31] are shown. The relative densities ρ/ρ_0 were obtained from Refs. 12 and 13, where ρ_0 is the 1/23.2 mol/cm^3 density of solid H_2 at 4.2 K and 1 bar. A single smooth curve fits through all of the data.

The dimensionless ratio $\Delta H/kT_{melt}$ varies between 10 and 35 for a wide variety of solids.[17] For similar solids (e.g., molecular solids with orientation disorder), the range is narrower. In fact, $\Delta H/kT_{melt}$ has been found to be independent of pressure for molecular solids such as hexamethylethane and cyclohexane.[19] However, the reported 2.8-kbar pressure range causes only a $\sim$30% change in T_{melt}. In Fig. 5, we present $\Delta H/kT_{melt}$ for solid H_2, covering a density range of 3 and a melting temperature range of 25. The low-density data[31] have ±10% error bars. The value of $\Delta H/kT_{melt}$ increases slowly and smoothly with pressure. The absence of a larger or sharper variation suggests that the same diffusion mechanism is present over a remarkably wide range of conditions.

The molecular jump rate ω_j may be computed from the motionally narrowed T_2 values using[19]

$$T_2^{-1}=0.9M_2/\omega_j \ . \tag{2}$$

This refers to the adiabatic limit $\omega_j \ll \omega_0$ which applies here (ω_0 is the spin precession frequency). The second moment M_2 refers only to intermolecular interactions. We make the standard assumptions that the molecules rotate spherically and without correlation between neighbors. It has been shown in this case that the correct intermolecular second moment M_2 is obtained by locating all the spins at the centers of the molecules.[38] Thus, for H_2 with 75% ortho-H_2 molecules with nuclear spin $I=1$, the powder average M_2 is[19,39]

$$M_2=\tfrac{3}{5}\gamma^4\hbar^2 I(I+1)\tfrac{3}{4}\sum_k (1/r_{jk}^6) \ . \tag{3}$$

For hcp H_2 at the density corresponding to 33 kbar at the melt, Eq. (3) yields $M_2=1.56\times10^{10}$ s^{-2}. Using this value of M_2 and the T_2 value from Fig. 3 extrapolated to infinite temperature (Table I), $T_2^\infty=8.5\times10^4$ s, the value of molecular jump rate extrapolated to infinite temperature is $\omega_j^\infty=1.2\times10^{15}$ s^{-1}. This is an acceptable value of the attempt frequency ω_j^∞ and indicates that our analysis is reasonable. Values of ω_j^∞ for other pressures are listed in Table I.

The values of T_2 in Fig. 3 have also been extrapolated to give values at the melting temperatures. Using Eq. (2) and second moments from Eq. (3) with densities from Refs. 12 and 13, molecular jump rates ω_j at the melt are determined. The jump rates at the melt are plotted in Fig. 6 and listed in Table I as a function of pressure, along with a zero-pressure datum.[31] The rate of jumps at the melt varies relatively little (after removing scatter) while the melting temperature varies by about 25. It has been proposed[40] that the rate of diffusion is a function only of the reduced temperature T/T_{melt}. The H_2 data of

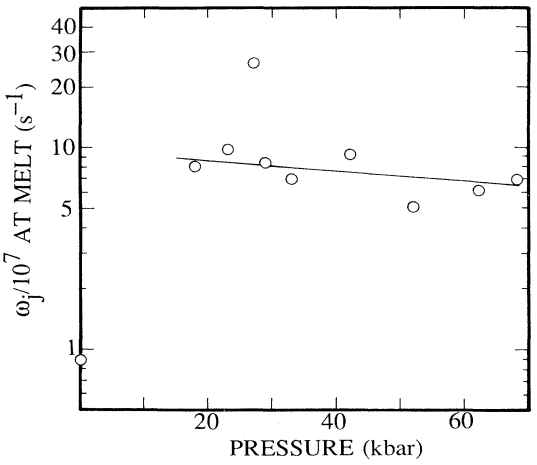

FIG. 6. Rate of molecular diffusion jumps ω_j at the melting temperature as a function of pressure. The high-pressure data are from this work; the zero-pressure datum is from Ref. 51. The line is an eye guide.

Fig. 6 provide remarkable support for this view, because of the wide range of melting temperature included.

The measured and derived values relating to self-diffusion in H_2 are summarized in Table I.

The spin-lattice relaxation time T_1 is presented in Fig. 7 as a function of temperature for two pressures. The regions of two-phase coexistence are shown by cross-hatching. In the solid near the melt, T_1 decreases because of the rapid diffusion modulation of the intermolecular dipole interactions. This behavior is identical to that observed in several molecular solids[19] and, in particular, solid H_2 at low pressure.[21] Well below the melting temperature, T_1 appears to be temperature independent and presumably reflects only molecular reorientations.

The observed relaxation rate T_1^{-1} can be expressed as a sum of two terms,

$$T_1^{-1}=T_{1\,\mathrm{rot}}^{-1}+T_{1\,\mathrm{diff}}^{-1}\ . \tag{4}$$

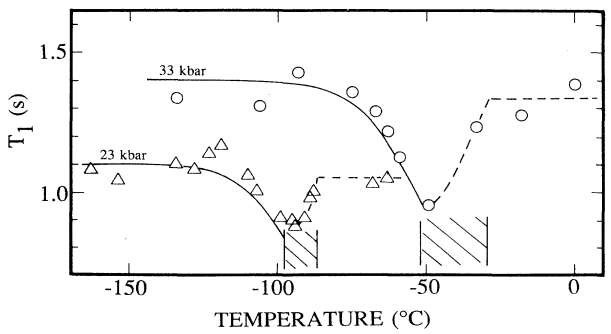

FIG. 7. Spin-lattice relaxation time T_1 as a function of temperature at two pressures. The melting regions are shown by cross-hatching. Just below the melting temperature, relaxation from diffusion decreases T_1. At lower temperatures the relaxation is from molecular reorientation only. The dashed lines are eye guides and the solid curves are from Eqs. (4) and (6).

The rate from translational diffusion may be written in the slow jump limit ($\omega_j \ll \omega_0$),[19]

$$T_{1\,\mathrm{diff}}^{-1}=2.3M_2\omega_j/\omega_0^2\ . \tag{5}$$

Combining Eq. (5) with Eq. (2), one obtains

$$T_{1\,\mathrm{diff}}^{-1}=2.1M_2^2T_2/\omega_0^2\ . \tag{6}$$

Using the 1.56×10^{10} s^{-2} value of M_2 for 33 kbar, $T_{1\,\mathrm{diff}}^{-1}$ was calculated from the measured T_2. Assuming a constant value of $T_{1\,\mathrm{rot}}=1.4$ s as measured and using Eq. (4) to add the relaxation rates, we obtain the solid curve in Fig. 7. A similar curve appears for 23 kbar. The good agreement with the data demonstrates that the decrease in T_1 below the melt indeed arises from diffusion.

The density dependence of the relaxation time $T_{1\,\mathrm{rot}}$ is displayed in Fig. 8. The low-density datum[21] is for 75% ortho-H_2 at 1 bar and 10 K. We believe our samples remained at 75% ortho-H_2 fraction because the conversion rate is expected to be low at high densities.[41] Also, our temperature range of 120–330 K is high enough that the equilibrium concentration varies only from 65 to 75 %.[20] The straight line fit to the data corresponds to $T_1 \propto \rho^{5/3}$. Since the molecular reorientation rate ω_{rot} certainly exceeds the nuclear spin resonance frequency ω_0, we have $T_1 \propto \omega_{\mathrm{rot}}$ and thus $\omega_{\mathrm{rot}} \propto \rho^{5/3}$. The electrostatic interaction between the molecular quadrupoles (EQQ) varies as r^{-5} and, therefore, $\rho^{5/3}$. Thus it appears that EQQ interactions cause molecular reorientations at the elevated densities and temperatures of this work as well

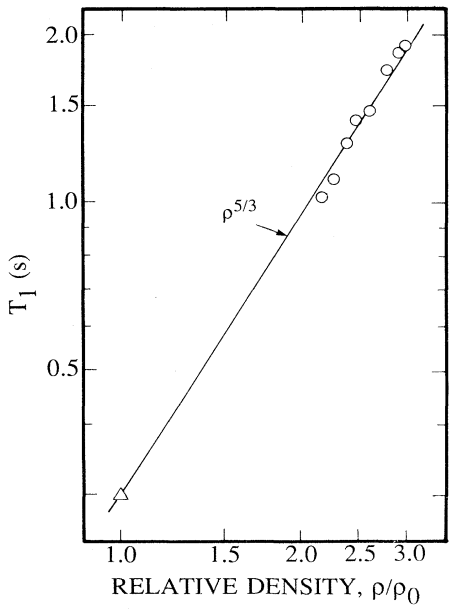

FIG. 8. The spin-lattice relaxation time T_1 due to reorientation as a function of relative density. The T_1 values are from the temperature-independent region well below the melt (see Fig. 7). The low-density datum is from Ref. 21 and refers to H_2 at 10 K, 1 bar, and 75% ortho-H_2 concentration. The straight line corresponds to $T_1 \propto \rho^{5/3}$.

as at low density and temperature. The large density range makes zero-point motion corrections to EQQ unimportant.

We note that in a previous study[42] of H_2 at pressures up to 7 kbar at 4.2 K, T_1 increased only as $\rho^{1.25}$. The sample had an ortho-H_2 fraction of 18%. At such relatively low densities (1.0–1.6) one expects the EQQ interactions to be dominant, as shown by the Raman work of Durana and McTague.[43] This should result in $T_1 \propto \rho^{5/3}$; we do not understand the density dependence observed by the Duke group.

At 300 K, 12% of the ortho-H_2 molecules are in the $J=3$ level. Fedders has calculated[44] the effect of the $J=3$ fraction upon T_1 for the case of phonon-induced reorientation (i.e., dilute ortho-H_2). However, there are no calculations relevant to the present situation of EQQ-induced reorientations. Our only estimate of the effect is from Fedders;[45] the fractional effect upon T_1 should be no longer than the fractional concentration of $J=3$.

A second effect of the high temperatures used in this work is that the para-H_2 molecules are not all in the $J=0$ state. Being spherically symmetric, the $J=0$ molecules serve as an inert diluent for the ortho-H_2 molecular spins. At 250 K, 39% of the para-H_2 are in the $J=2$ state. These $J=2$ molecules can couple to the $J=1$ molecules and induce mutual Δm_J transitions. One expects that the net effect of the $J=2$ population will be to increase the effective concentration of $J\neq 0$ molecules, increasing the reorientation rate $\omega_{\rm rot}$ and T_1. The magnitude of this change will depend upon the $J=2$ lifetime compared to the characteristic time for Δm_J transitions. For example if the $J=2$ lifetime is short, mutual Δm_J transitions between a $J=2$ and a $J=1$ will be interrupted. In the limit of very short $J=2$ lifetimes, the $J=2$ population will have no effect upon the dynamics of the $J=1$ molecules. Since no calculations of these effects are available, we can only alert the reader to the uncertainties in the above analysis leading to $T_1 \propto \rho^{5/3}$. On the other hand, at 150 K only 14% of the para-H_2 are $J=2$, so the effect upon T_1 should be small. The good fit in Fig. 8 to the $\rho^{5/3}$ dependence is an indication that the total influence of higher J states is not substantial.

At sufficiently high densities, the anisotropic parts of molecular attraction and repulsion should become important. Only at large separations is the EQQ with its r^{-5} dependence the dominant anisotropic interaction. The $\rho^{5/3}$ dependence of the rotational T_1 indicates that EQQ dominates even at $\rho/\rho_0=3$. We note previous work indicated that EQQ is the main anisotropic interaction in H_2 up to relative densities of 1.56 (Ref. 43) and 1.7.[46] A phase transition was observed at 77 K and 1450 kbar;[47] it was interpreted as the hcp-Pa3 orientational ordering transition at relative density 8. The transition temperature scaled as $\rho^{5/3}$ from low-density data, suggesting that EQQ interactions dominate even at this very high density. Recently the temperature and ortho-concentration dependences of the transition pressure have been measured[38] and are in disagreement with the interpretation of the transition as orientational ordering.

At low concentrations of ortho-H_2, a phonon-rotation coupling was observed for H_2 in Ne, Ar, and Kr as well as in para-H_2 host.[49] This coupling causes a phonon-induced reorientation rate $\Gamma_{\rm ph}$. The temperature dependence of $\Gamma_{\rm ph}$ (T^2 at high temperatures and T^7 at low temperatures) indicates a two-phonon Raman process. A T^2 extrapolation of the H_2 in argon data yields an expected $\Gamma_{\rm ph}=1.8\times10^{11}$ s^{-1} at 300 K. (The H_2 in argon data are more complete than the H_2 in para-H_2 data, but are approximately equal where they overlap. Of course, the H_2 host in the present work has been stiffened by pressure, so the value of $\Gamma_{\rm ph}$ is only an estimate.) The observed $T_{1\,\rm rot}$ at 62 kbar of 1.8 s can be used to estimate the total (from all sources) rate $\omega_{\rm rot}$ of molecular reorientation. Using Fedders' language, $\omega_{\rm rot}$ equals Γ_2; assuming the cubic symmetry case, we have[50]

$$T_1^{-1}=18.1\omega_d^2/\omega_{\rm rot}\ . \tag{7}$$

Using Fedders' numerical values, Γ_2 is given by

$$\omega_{\rm rot}=2.37T_1\times10^{12}\ {\rm s}^{-1}\ , \tag{8}$$

where T_1 is in seconds. Thus at 62 kbar the reorientation rate $\omega_{\rm rot}=4.3\times10^{12}$ s^{-1}. This is considerably larger than the estimated phonon contribution. Thus the observed independence of $T_{1\,\rm rot}$ upon temperature is explained.

IV. CONCLUSIONS

We have presented proton NMR data on molecular self-diffusion and reorientation in solid H_2 at diamond anvil cell pressures. The activation enthalpy ΔH of diffusion increases with pressure, yielding an activation volume of 5.7 ± 0.6 cm^3/mol. This volume is 63% of the molar volume, a reasonable value for the monovacancy diffusion mechanism. The variation of $\Delta H/kT_{\rm melt}$ with density is slow and smooth, suggesting that a single mechanism controls diffusion over the range $\rho/\rho_0=1$ to 3. The spin-lattice relaxation time T_1 arising from molecular reorientation is independent of temperature and varies as $\rho^{5/3}$. This indicates that the EQQ interaction dominates molecular reorientation (Δm_J transitions) over the range $\rho/\rho_0=1$ to 3. Other anisotropic molecular interactions of shorter range as well as coupling to the phonons are not effective.

ACKNOWLEDGMENTS

This work was supported in part by NSF Grant No. DMR 87-02847 and one of us (R.E.N.) was supported by NSF Grant No. DMR 87-01515. The early stages of the research were supported in part through the generosity of the donors to the Petroleum Research Fund, administered by the American Chemical Society. We benefited from conversations with D. Schiferl, I. Silvera, and P. A. Fedders.

[1]R. M. Hazen, H. K. Mao, L. W. Finger, and R. J. Hemley, Phys. Rev. B **36**, 3944 (1987).
[2]B. Olinger, R. L. Mills, and R. B. Roof, Jr., J. Chem. Phys. **81**, 5068 (1984).
[3]R. L. Mills, B. Olinger, and D. T. Cromer, J. Chem. Phys. **84**, 2837 (1986).
[4]J. F. Mammone, S. K. Sharma, and M. Nicol, J. Phys. Chem. **84**, 3130 (1980).
[5]S. Buchsbaum, R. L. Mills, and D. Schiferl, J. Phys. Chem. **88**, 2522 (1984).
[6]D. Schiferl, S. Kinkead, R. C. Hanson, and D. A. Pinnick, J. Chem. Phys. **87**. 3016 (1987).
[7]H. D. Hochheimer, H. J. Hodl, W. Henkel, and F. Bolduan, Chem. Phys. Lett. **106**, 79 (1984).
[8]R. Reichlin, D. Schiferl, S. Martin, C. Vanderborgh, and R. L. Mills, Phys. Rev. Lett. **55**, 1464 (1985).
[9]J. van Straaten and I. F. Silvera, Phys. Rev. Lett. **57**, 766 (1986).
[10]S.-H. Lee, K. Luszczynski, R. E. Norberg, and M. S. Conradi, Rev. Sci. Instrum. **58**, 415 (1987).
[11]V. Diatschenko and C. W. Chu, Science **212**, 1393 (1981); a small extrapolation of the data was performed.
[12]A. Driessen and I. F. Silvera, J. Low Temp. Phys. **54**, 361 (1984).
[13]J. van Straaten, R. J. Wijngaarden, and I. F. Silvera, Phys. Rev. Lett. **48**, 97 (1982).
[14]C. P. Flynn, *Point Defects and Diffusion* (Clarendon, Oxford, 1972).
[15]H. A. Reich, Phys. Rev. **129**, 630 (1963).
[16]G. J. Dienes, J. Appl. Phys. **23**, 1194 (1952).
[17]R. J. Borg and G. J. Dienes, *An Introduction to Solid State Diffusion* (Academic, New York, 1988).
[18]K. C. Pandey, Phys. Rev. Lett. **57**, 2287 (1986).
[19]N. Boden, in *The Plastically Crystalline State,* edited by J. N. Sherwood (Wiley-Interscience, New York, 1979).
[20]I. F. Silvera, Rev. Mod. Phys. **52**, 393 (1980).
[21]F. Weinhaus and H. Meyer, Phys. Rev. B **7**, 2974 (1973).
[22]A. Jayaraman, Rev. Mod. Phys. **55**, 65 (1983).
[23]A. Jayaraman, Rev. Sci. Instrum. **57**, 1013 (1986).
[24]Tico Titanium, Inc., Farmington Hills, Michigan.
[25]Rhenium Alloys, Inc., P.O. Box 245, Elyria, Ohio 44036.
[26]D. Schiferl (private communication).
[27]J. D. Barnett, S. Block, and G. J. Piermarini, Rev. Sci. Instrum. **44**, 1 (1973).
[28]I. F. Silvera and R. J. Wijngaarden, Rev. Sci. Instrum. **56**, 121 (1985).
[29]R. L. Mills, D. H. Liebenberg, J. C. Bronson, and L. C. Schmidt, Rev. Sci. Instrum. **51**, 891 (1980).
[30]C. P. Slichter, *Principles of Magnetic Resonance* (Springer, New York, 1980).
[31]G. W. Smith and C. F. Squire, Phys. Rev. **111**, 188 (1958).
[32]N. H. Nachtrieb and C. Coston, in *Physics of Solids at High Pressure,* edited by C. T. Tomizuka and R. M. Emrick (Academic, New York, 1965), p. 336.
[33]J. N. Sherwood, in *The Plastically Crystalline State,* edited by J. N. Sherwood (Wiley-Interscience, New York, 1979).
[34]J. M. Chezeau and J. H. Strange, Phys. Rep. **53**, 1 (1979).
[35]J. H. Strange and S. M. Ross, Mol. Cryst. Liq. Cryst. **32**, 67 (1976).
[36]W. C. Allen, N. Liu, and J. Jonas, J. Chem. Phys. **63**, 3317 (1975).
[37]R. Folland, S. M. Ross, and J. H. Strange, Mol. Phys. **26**, 27 (1973).
[38]L. V. Dmitrieva and V. V. Moskalev, Fiz. Tverd. Tela (Leningrad) **5**, 2230 (1963) [Sov. Phys.—Solid State **5**, 1623 (1964)].
[39]A. Abragam, *The Principles of Nuclear Magnetism* (Clarendon, Oxford, 1961).
[40]N. H. Nachtrieb, H. A. Resing, and S. A. Rice, J. Chem. Phys. **31**, 135 (1959).
[41]A. Driessen, E. van der Poll, and I. F. Silvera, Phys. Rev. B **30**, 2517 (1984).
[42]P. L. Pedroni, R. Schweizer, and H. Meyer, Phys. Rev. B **14**, 896 (1976).
[43]S. C. Durana and J. P. McTague, Phys. Rev. Lett. **31**, 990 (1973).
[44]P. A. Fedders, Phys. Rev. B **30**, 3603 (1984).
[45]P. A. Fedders (private communication).
[46]I. F. Silvera and R. Jochemsen, Phys. Rev. Lett. **43**, 377 (1979).
[47]R. J. Hemley and H. K. Mao, Phys. Rev. Lett. **61**, 857 (1988).
[48]H. E. Lorenzana, I. F. Silvera, and K. A. Goettel, Phys. Rev. Lett. (to be published).
[49]M. S. Conradi, K. Luszczynski, and R. E. Norberg, Phys. Rev. B **20**, 2594 (1979).
[50]P. A. Fedders, Phys. Rev. B **20**, 2588 (1979).
[51]M. Bloom, Physica **23**, 767 (1957).